# The Effect of Internal Pipe Wall Roughness on the Accuracy of Clamp-On Ultrasonic Flowmeters

Xiaotang Gu and Frederic Cegla

***Abstract*— Clamp-on transit-time ultrasonic flowmeters (UFMs) suffer from poor accuracy compared with spool-piece UFMs due to uncertainties that result from the in-field installation process. One of the important sources of uncertainties is internal pipe wall roughness which affects the flow profile and also causes significant scattering of ultrasound. This paper purely focuses on the parametric study to quantify the uncertainties (related to internal pipe wall roughness) induced by scattering of ultrasound and it shows that these effects are large even without taking into account the associated flow disturbances. The flowmeter signals for a reference clamp-on flowmeter setup were simulated using 2-D finite element analysis including simplifying assumptions (to simulate the effect of flow) that were deemed appropriate. The validity of the simulations was indirectly verified by carrying out experiments with different separation distances between ultrasonic probes. The error predicted by the simulations and the experimentally observed errors were in good agreement. Then, this simulation method was applied on pipe walls with rough internal surfaces. For ultrasonic waves at 1 MHz, it was found that compared with smooth pipes, pipes with only a moderately rough internal surface (with 0.2-mm rms and 5-mm correlation length) can exhibit systematic errors of 2% in the flow velocity measurement. This demonstrates that pipe internal surface roughness is a very important factor that limits the accuracy of clamp on UFMs.**

***Index Terms*— Clamp-on flowmeter, roughness, transit time, ultrasound, uncertainties.**

## I. Introduction

TRANSIT-time ultrasonic flowmeters (UFMs) are widely used in many industrial sectors, such as oil and gas, power, nuclear, process, water distribution, and chemical plants. These flowmeters measure flow velocity by calculating the difference in arrival time between the ultrasonic signals that are traveling with the flow (downstream signal) and against the flow (upstream signal). There are two common ways to install the ultrasonic transducers, "inline" and "clamp-on" (Fig. 1). The installation of the inline UFM requires cutting the pipe and subsequent insertion of a premanufactured and calibrated spool piece that contains integrated ultrasonic transducers. The clamp-on flowmeter only requires transducers to be mounted on the outside of the pipe wall to take a measurement. This clamp-on flowmeter has a number of advantages compared with other flowmeters. It is noninvasive, easy to install, and requires a little maintenance [1].

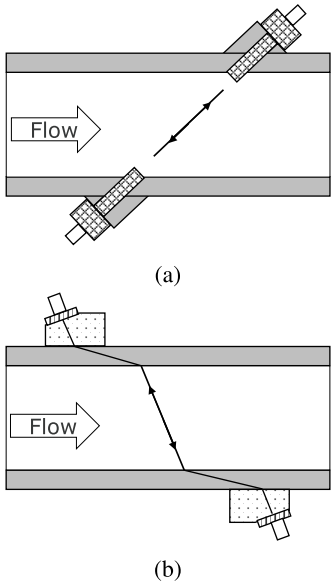


Fig. 1. (a) Direct path inline transit-time UFM. (b) Direct path clamp-on transit-time UFM. The black bar is the pipe wall. The black dotted shape is the transducer and the angled wedge. The arrows represent ultrasonic propagation path.

While the clamp-on transit-time UFM has many advantages, its main disadvantage is the uncertainties that are a result of the in-field installation process [2]. The source of uncertainties may come from installation of transducers, pipe works, properties of fluid, and so on, among which some of the sources have been studied, such as inhomogeneity of pipe materials [3], separation distance between transducers [4], and frequency of transducers [5]. However, there is a limited amount of information available on the effect of internal pipe wall roughness on the uncertainties. The pipe wall roughness would induce uncertainties in two sets of problems, one is distortion of the flow profile, the other is the scattering of ultrasound [6]. The flow profile has been studied by Mori *et al.* [7] and Calogirou *et al.* [8], but there are limited studies on the scattering of ultrasound from rough surfaces on flow measurements. Szebeszczyk's research [9] shows that the deposits on the internal pipe wall cause large attenuation and distortion of the received ultrasound signal. Cermakova *et al.* [10] demonstrate the impact of the roughness of the pipe by comparing measurements on corroded and noncorroded pipes. However, these studies only show that pipe wall roughness has a large impact. None of these studies

Manuscript received January 24, 2018; revised March 28, 2018; accepted April 19, 2018. Date of publication May 16, 2018; date of current version December 7, 2018. This work was supported by ABB. The Associate Editor coordinating the review process was Dr. V. R. Singh. *(Corresponding author: Frederic Cegla.)*

The authors are with the Non-Destructive Evaluation Group, Mechanical Engineering, South Kensington Campus, Imperial College London, London SW7 2AZ, U.K. (e-mail: xg910@imperial.ac.uk; f.cegla@imperial.ac.uk).

Color versions of one or more of the figures in this paper are available online at http://ieeexplore.ieee.org.

Digital Object Identifier 10.1109/TIM.2018.2834118

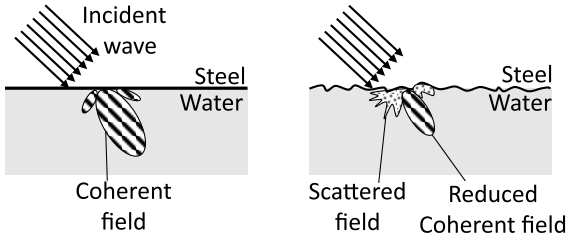


Fig. 2. Schematic changes in scattered energy distribution using polar plots. (a) Smooth surface. (b) Rough surface. The rough surface reduces the energy of the transmitted coherent field and increases the scattered energy.

provide a parametric study to quantify the range of the possible errors caused by different roughness parameters due to scattering. Wave scattering from a rough surface has been the subject of study for many decades [11]. As can be seen in Fig. 2, the rougher the surface, the higher the reduction in the energy of the transmitted coherent field will be. This can cause phase modulation and attenuation [12] of the received signal. For flow measurements in the field, this may potentially reduce the signal-to-noise ratio and cause distortion of the signal waveform. Since the internal pipe wall is inevitably rough, the impact of the wave scattering from these surfaces needs to be studied and quantified.

Therefore, the aim of this paper is to carry out parametric studies to quantify the effect that internal pipe wall surface roughness has on the uncertainties of clamp-on UFMs for nonflow profile related effects (scattering effects).

To achieve this, a reference simulation method (with simplifying assumptions which were deemed suitable) is presented in Section II. This simulation method was then verified experimentally by quantifying uncertainties that result from horizontal separation between transducer probes (Section III). Then, the method was used to quantify the effect of internal pipe wall roughness on uncertainties for different roughness parameters (Section IV).

## II. Reference Simulation Method

### A. Static Reference Condition

Fig. 3 shows the reference setup of a typical direct path clamp-on UFM. The main components in this setup are the pipe, fluid, wedges, and transducers. The transducers are placed onto the angled edge of the perspex wedges which are clamped onto the opposite sides of the steel pipe wall. This setup allows the two transducers to send ultrasound to each other at an oblique angle to the flow direction. The properties of each component are shown in Table I. Water is chosen as the fluid, and the pipe size follows the industry standard [13].

The selection of the wedge angle has to satisfy two criteria, to maximize the velocity sensitivity and also to ensure that only shear waves exist in the pipe wall so that only one beam of ultrasound propagates in water [5]. To maximize velocity sensitivity, the propagation angle ($\theta$) of ultrasound in water needs to be maximized. To ensure that only shear waves exist in the pipe wall, $\theta$ has to be larger than the first critical angle and less than the second critical angle. According to

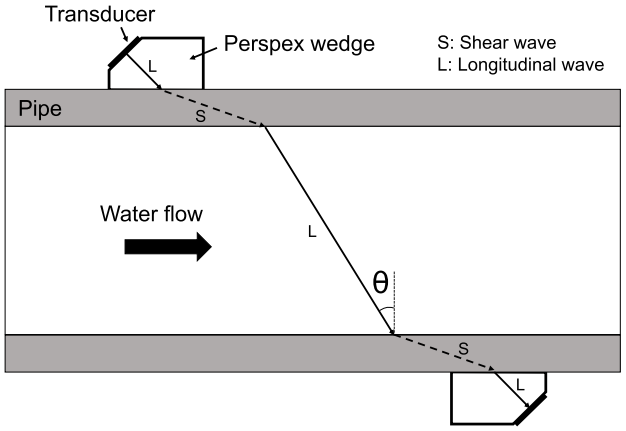


Fig. 3. Illustration of the reference condition. Pipe, fluid, and wedge properties are shown in Table I. $\theta$ is the propagation angle in water.

TABLE I
Properties of the Steel Pipe, Water and Wedge for the Reference Condition

| Properties | Nominal Value |
|---|---|
| Pipe properties | |
| Standard | $3^1/_2$ NPS, SCH 40s |
| Outer diameter (mm) | 101.6 |
| Thickness (mm) | 5.74 |
| Material | Carbon steel |
| Young's modulus (GPa) | 217 |
| Material Density ($kg/m^3$) | 7932 |
| Water flow properties | |
| Temperature (°C) | 20 |
| Density ($kg/m^3$) | 998.2 |
| Bulk modulus (GPa) | 2.17 |
| Average flow velocity(m/s) | 2 |
| Reynold's Number | 1.8x10$^5$ |
| Perspex wedge properties | |
| Wedge angle(°) | 50 |
| Wedge thickness (mm) | 20 |
| Young's modulus (GPa) | 6.33 |
| Density ($kg/m^3$) | 1180 |

Snell's law, (1) calculates the range of $\theta$, where $c_{sl}$ and $c_{ss}$ are the shear and longitudinal wave velocity in steel pipe and $c_w$ is the phase velocity in water. Using the information in Table I, $\theta$ was calculated to be between 14° and 27°. However, to allow for the uncertainty in material properties, an angle of approximately 24° was chosen. This provides some slack and also results in a nice round angle of 50° for the perspex wedge. These values are similar to those encountered in some industrial applications [14]

$$\arcsin \frac{c_w}{c_{sl}} < \theta < \arcsin \frac{c_w}{c_{ss}}. \tag{1}$$

After $\theta$ has been fixed, Snell's law was used to determine the propagation angle in all three media and then the installation horizontal distance (ideal installation distance) between the wedges (transducers) was calculated. This distance is used as the separation distance of the wedges for the reference condition.

TABLE II

DETAILS OF ELEMENT AND MESH CHOICE FOR A FULL-SCALE 2-D CLAMP-ON FLOWMETER FEM. 2-D ACOUSTIC ELEMENTS ARE USED TO MODEL WATER AND 2-D SOLID ELEMENTS ARE USED TO MODEL THE WEDGE. THE MESH SIZE WAS SELECTED SUCH THAT AT LEAST 15 ELEMENTS PER WAVELENGTH WERE USED. CPE4R IS A FOUR-NODE BILINEAR PLANE STRAIN QUADRILATERAL ELEMENT AND AC2D4R IS A FOUR-NODE LINEAR 2-D ACOUSTIC QUADRILATERAL ELEMENT

| Layer | Perspex wedge | Steel pipe | Water |
|---|---|---|---|
| Element type | CPE4R | CPE4R | AC2D4R |
| Mesh size (mm) | 0.05 | 0.1 | 0.05 |
| Minimum wavelength (mm) | 1.43 | 3.26 | 1.48 |
| No. elements per wavelength | 28.6 | 32.6 | 29.6 |

### B. FE Simulation

After defining the reference condition, a finite element model (FEM) was setup using the commercial software, Abaqus/Explicit. This solver is based on integration of the equations of motion for the body using an explicit central difference integration rule [15]. The setup of the full-size model is shown in Fig. 4. The dimensions of each layer were as described in the reference condition. One of the transducers was modeled as the generator and the other one as the receiver. The generator signal was a Hanning windowed toneburst with 1-MHz, five cycles in the time domain, and a Gaussian beam in the space domain. The amplitude of the central displacement on the generator transducer was 1 $\mu$m.

To accurately model the wave propagation, it is necessary to ensure correct element size and time step size in order to ensure accuracy and stability. According to [16], the choice of 15 elements per wavelength should have enough mesh density for modeling, so the mesh size ($\Lambda$) was calculated accordingly using (2)

$$\Lambda \leqslant \frac{\lambda_{\min}}{N_e} \tag{2}$$

where $N_e$ is the minimum number of elements per wavelength. The selection of element and mesh size are shown in Table II. In addition, to ensure the stability of the model, the time step ($t_s$) is calculated using (3) as suggested by Abaqus/Explicit

$$t_s < \frac{\Lambda}{c_{\max}} \tag{3}$$

where $c_{\max}$ is the maximum phase velocity in the model. In this case, the maximum phase velocity is the longitudinal velocity in steel and therefore the choice of ts $=$ 5 ns is resulted.

Fig. 5 shows the sum of the displacement magnitude of all the observation points on the receiver transducer. It can be seen that there are no signals before the first longitudinal wave arrives. Furthermore, shear waves arrive immediately after the longitudinal wave. This is expected because the shear wave (second 'S' wave in Fig. 3) incident on the steel–perspex interface will generate both longitudinal and shear transmission in the perspex wedge.

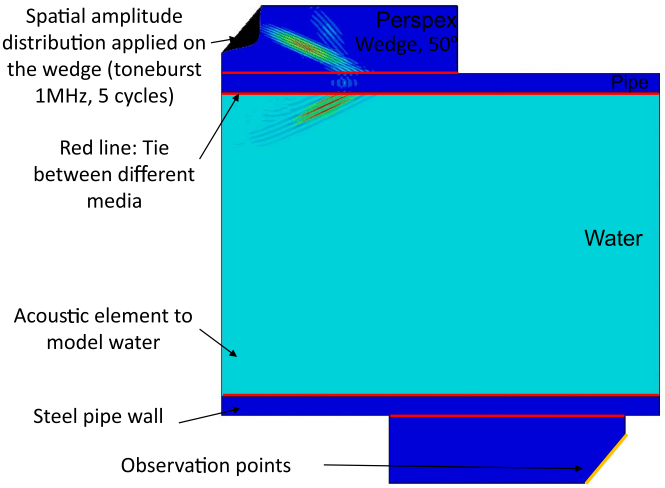


Fig. 4. FE model setup in Abaqus, showing the stress wave in the perspex wedge and steel pipe and the acoustic pressure wave in the water, 18 $\mu$s after the transducer emits the signal. An arbitrary and different color map scale was chosen to visualize both the stress and acoustic pressure wave on the same plot. The pipe and wedge are using the same color scale (rainbow) to represent the displacements due to the ultrasonic wave in these two media, where blue represents low or no displacement and red represents large displacement. The wave in the water is shown in the form of the acoustic pressure and this is hence potted on a different color scale.

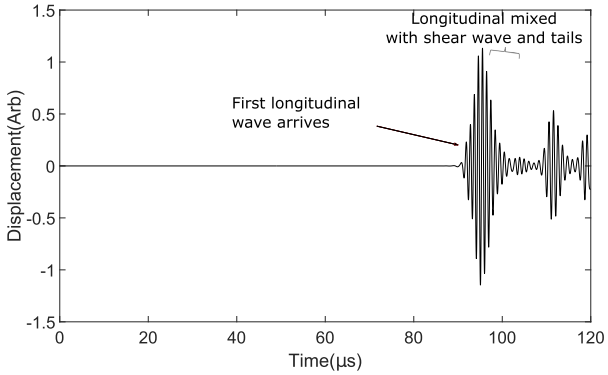


Fig. 5. Reference signal transmitted through pipe without flow.

### C. Flow Simulation

After defining and modeling the static reference condition, the flow and both upstream and downstream signals needed to be simulated. A number of simulation methods have been published to simulate the flow in a UFM using ray tracing [17], FEM [18], and commercial CFD software [19]. These flow simulation methods are computationally demanding and a single simulation may take up to one day. In addition, the focus of these papers was to investigate the effect of the flow on the receiving signals, whereas the focus of this paper is to investigate the effect of roughness (parametric study) on flow measurement uncertainties. Therefore, to optimize simulation speed, a simplified method to simulate the effect of flow was used in this paper based on considerations of what happens in the fluid. Without flow, as shown in Fig. 6(a), the ultrasonic wave packet with phase angle $\alpha$ propagates at the same angle $\alpha$ and arrives at the other end of the pipe at the same phase angle $\alpha$. Assuming uniform flow across the cross section of the pipe (Fig. 6), while the phase angle of the wave packet

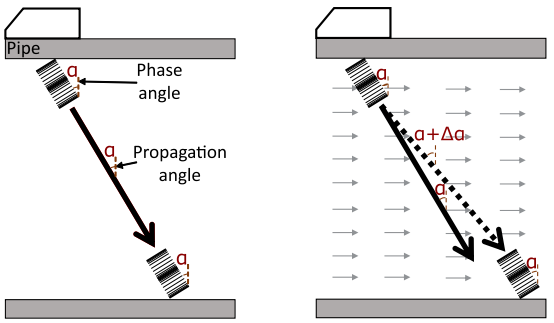


Fig. 6. Effect of the flow on ultrasonic wave propagation. The transducer sends ultrasonic signals through the pipe and arrives at the other side of the pipe. To a first approximation, the phase angle remains the same, whereas the angle at which the wave packet traverses the pipe changes. (a) Propagation of ultrasound without flow. (b) Propagation of ultrasound with uniform flow.

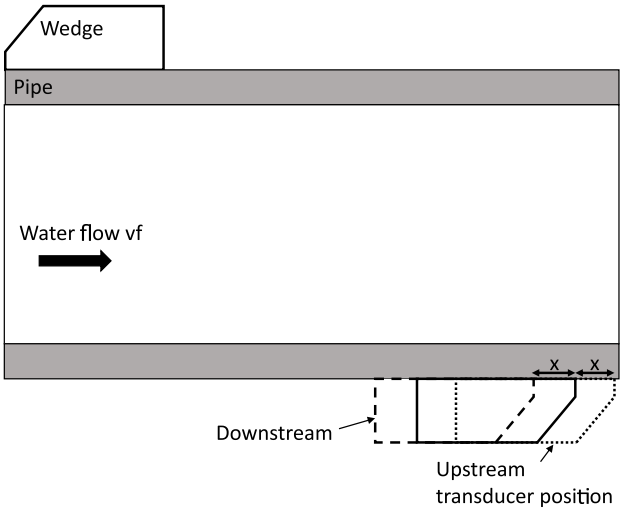


Fig. 7. Transducer movement to simulate flow and shift of the location at which the wave packet arrives on the other side of the pipe.

with respect to the pipe cross section remains the same (the impedance mismatch between the pipe and water remains constant), the angle at which the wave packet traverses the pipe cross section changes to $\alpha + \delta\alpha$. The same phenomenon was observed in [19].

This suggests that the upstream and downstream signals can be simulated by moving the receiving transducer along the pipe wall at a distance $x$ [see (4)] while maintaining the transmitting transducer at the same location. This is illustrated in Fig. 7

$$x = V_f \frac{l_w}{c_w} \tag{4}$$

where Vf is the flow velocity, $l_w$ is the travel distance in water, and $c_w$ is the phase velocity of ultrasound in water. Fig. 8 shows the upstream and downstream signals that are simulated using this method.

This method not only keeps the complexity of signals by taking into account the presence of both shear and longitudinal waves but also reduces the required computation effort. The assumptions that a uniform flow profile exists and that the phase angle of the wave packet remains the same with respect to the pipe cross section (with or without the flow) were made.

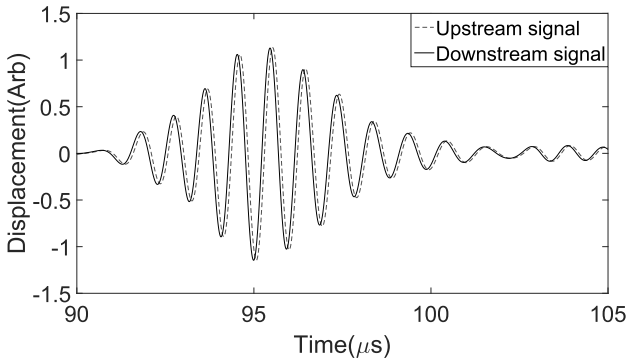


Fig. 8. Simulated upstream and downstream signals.

TABLE III
SIGNAL PROCESSING METHOD TO DETERMINE FLOW VELOCITY FROM SIMULATED SIGNALS

| Steps | Procedure |
|---|---|
| 1 | The upstream and downstream signals are digitally filtered using a 5th order Butterworth filter with cut-off frequency 0.6MHz and 1.4MHz. |
| 2 | The signal tail which is defined to start 5 cycles after the maximum in signals is removed |
| 3 | The upstream and downstream signals are cross-correlated. |
| 4 | The signal is zero-padded in the frequency domain so that a virtual sampling frequency of 800MHz is achieved |
| 5 | Linear interpolation is used between samples to find the maximum of the cross-correlation function and the arrival time difference ($\Delta t$). |
| 6 | The flow velocity is calculated using the transit time equation (Equation 5). |

### *D. Signal Processing Method to Determine Flow Velocity From Simulated Signals*

Table III shows the signal processing steps that were used to calculate flow velocity from the simulated upstream and downstream signals

$$vf = \frac{d_i \Delta t}{2 t_u t_d \sin\theta \cos\theta} \tag{5}$$

where $vf$ is the mean flow velocity, $\Delta t$ is the difference of the arrival time between $t_u$ (upstream arrival time) and $t_d$ (downstream arrival time), $d_i$ is the internal diameter of the pipe, and $\theta$ is the angle between the sound travel path in water and the normal direction. $vf$ can be determined by combining the individual upstream and downstream travel times that are shown in

$$t_u = \frac{d_i}{\cos\theta (c_w - vf \sin\theta)} \tag{6}$$

$$t_d = \frac{d_i}{\cos\theta (c_w + vf \sin\theta)} \tag{7}$$

where $t_u$ and $t_d$ are upstream and downstream arrival time, $c_w$ is the phase velocity in water, $vf$ is the mean flow velocity, and $d_i$ is the internal diameter of the pipe. The upstream signal is decelerated by the flow while the downstream signal is accelerated.

The cross-correlation function and interpolation were used to determine the arrival time difference. The correlation method is the best for cases with low S/N ratio, but the limiting

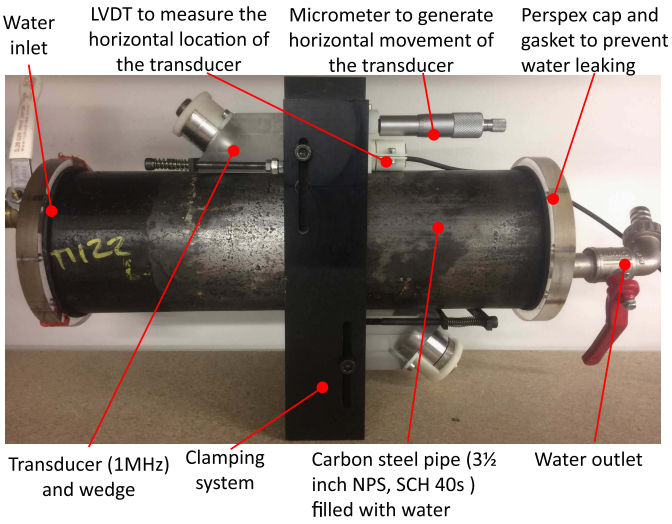


Fig. 9. Photograph of the transducers and pipe sample that were used in experiments.

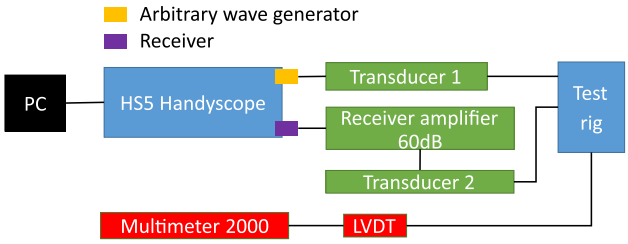


Fig. 10. Block diagram showing how the individual elements were connected together in the experimental setup.

factor is the sampling frequency which can be improved by interpolation [20], [21]. This processing method provides a reference method to process the signals and therefore allowing the parametric study to be performed unbiased.

## III. Verification Experiments

### A. Experimental Setup

An experimental setup as shown in Fig. 9 was built. The dimensions are the same as in Table I.

Transducers (Aerotech) with center frequency of 1 MHz were fixed by brackets onto a 50° angled perspex wedge. A micrometer was fixed onto the clamping system to move the wedge and transducer horizontally by small distances (accurate to 10 $\mu$m).

Furthermore, a linear variable differential transformer (LVDT VG/2/s, 54.1 mV/V/mm sensitivity, Solartron Metrology, West Sussex, U.K.) is used to measure the horizontal displacement of the wedge. In this case, a multimeter (61/2-Digit Multimeter 2000, KEITHLEY, Bracknell, U.K.) that has resolution 10-$\mu$V (able to condition the LVDT to repeatability of 0.018 $\mu$m), 10-V range was used to read the output of this LVDT. Therefore, if the distance required to move is 300$\mu$m in order to generate 2-m/s estimated flow, the theoretical repeatability of this distance measurement is better than 0.1%.

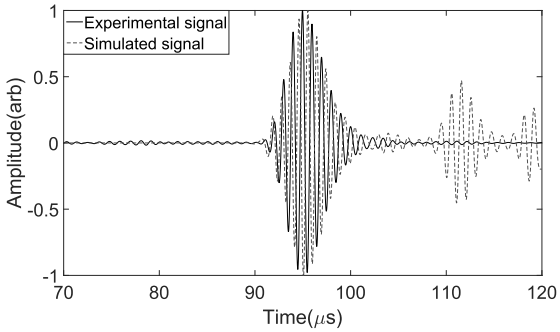


Fig. 11. Experimental reference signal compared with simulated reference signal.

A schematic electrical setup is shown in Fig. 10. The Handyscope HS5 (Tiepie Ltd., Sneek, The Netherlands) was used to transmit signals (1-MHz, five cycles toneburst, 12 V) via one of the transducers. The other transducer is used to receive the analog signal, which is amplified and digitized (14-bit ADC at 200-MHz sampling frequency) on one of the ports of the HS5.

Fig. 11 shows the static reference signal obtained experimentally (not moving the wedge). It can be seen that there is good agreement between the arrival time and wave shape of the simulated and experimental signal. There are also small discrepancies that can be noticed. Compared with the simulation signal, there are additional low-amplitude waves arriving before the main signal. This might be the waves traveling around the circumference of the pipe; while they would need to travel further, the speed of sound in the pipe is faster than in the liquid. Since the simulation is 2-D, there are no 3-D effects such as the curvature of the pipe being simulated. The tail of the signals is also different. In simulation, there are significant amounts of energy reflected from the top of the wedge which arrive later than the main signals, but these signals seem to be attenuated in the experiment.

### B. Horizontal Distance Uncertainty Test

For the purpose of verifying the simulation, the experimental setup was used to determine the uncertainties of one of the easily measured parameters, horizontal separation distance between the transducer probes.

Errors of horizontal distance were introduced deliberately by moving the receiver transducer relative to the reference condition. For each position (expressed as a % error with respect to the horizontal separation distance of the reference condition), the upstream and downstream signals were obtained by an additional small positioning offset with respect to the new horizontal transducer position, as previously described in Section II-C. Then, procedures in Table IV were carried out to obtain repeated flow measurements at one position.

The tests were repeated for horizontal distance errors from −40 to +30 mm.

The flow velocity error was then plotted against the error in the horizontal separation distance of the transducers. The negative distance error means that the wedges were closer to

TABLE IV
EXPERIMENTAL TEST PROCEDURE

| Steps | Procedure |
|---|---|
| 1 | The wedges were placed onto the pipe at a required horizontal separation distance |
| 2 | 50 ultrasonic signals were sent from one transducer to the other, these signals represent the downstream signal |
| 3 | One of the wedges was displaced horizontally (increasing the horizontal separation distance between the two transducer by $2x$) |
| 4 | Another 50 ultrasonic signals were sent, these signals represent the upstream signal |
| 5 | The upstream and downstream signal are processed to calculate the estimated flow velocity($v_s$). |
| 6 | Flow velocity error is calculated using $\frac{V_s - V_r}{V_r}$, where $V_r$ is the reference velocity |
| 7 | Procedures from 1 to 6 were repeated 10 times and the velocity errors were averaged |

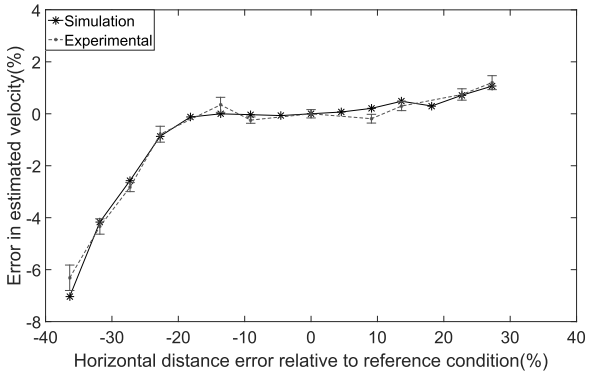


Fig. 12. Estimated flow velocity error as a function of horizontal separation distance error. The error bar represents the standard deviation of the estimated flow velocity measured experimentally.

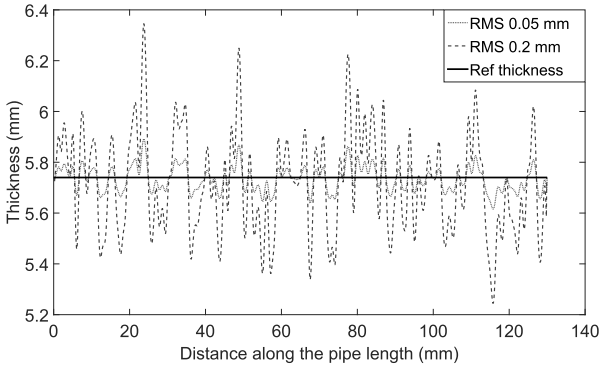


Fig. 13. Pipe roughness profile for the internal wall surface with different rms heights and correlation length 1 mm.

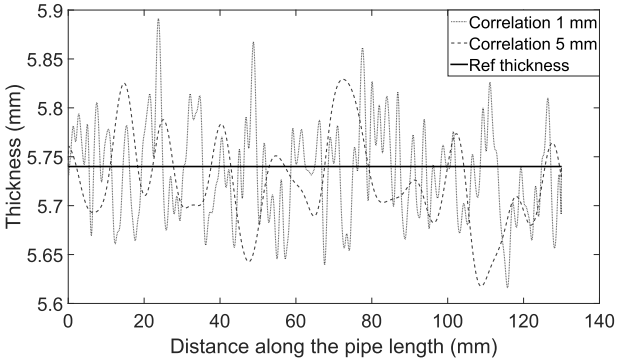


Fig. 14. Illustration of different correlation lengths used in the simulation of the effect of internal pipe wall roughness on uncertainties of clamp-on UFM with rms value 0.05 mm.

each other compared with the reference condition, whereas the positive distance error means that they were further apart.

Fig. 12 shows the result for this test. It can be seen that between $-15\%$ and 15% horizontal distance error, the velocity error estimated from simulations was small compared with the standard deviation in experimental tests. This means that if the horizontal distance error varies from $-15\%$ to 15%, the estimated errors cannot be accurately measured by the test setup and therefore cannot be proved that the experiments agree with simulation. However, outside this range, the simulations predicted that much larger errors could be experimentally confirmed. This gave us confidence that the presented simulation approach yields valid results.

## IV. PIPE ROUGHNESS UNCERTAINTY SIMULATION

After good agreement between simulation and experiment was found, this method was applied to investigate the effect of pipe roughness on uncertainties of UFMs. There are both external and internal pipe surfaces and they both can be rough. In this case, only the internal pipe roughness is considered as this is the surface that cannot be accessed during the installation process.

The surface roughness is defined using rms height (vertical extent) and correlation length (horizontal extent) [22]. Fig. 13 shows the examples of the surface profile for different rms values with reference to the reference thickness of the pipe (5.74 mm for $3\frac{1}{2}$-in NPS, SCH 40s pipe). A value of 0.05 mm is the estimated roughness for a new pipe, whereas 0.2 mm is the roughness for a moderately corroded pipe [23]. Correlation length is a statistical measure of the variation of the roughness profile along the pipe lengths. Fig. 14 shows the surface profiles of different correlation lengths. Three lengths were chosen, 1, 3, and 5 mm, where 3 mm is approximately the wavelength for 1 MHz shear wave ultrasound in the steel pipe.

Twelve different combinations of roughness parameters (rms value and correlation length) were simulated. For each combination, ten different realizations of thickness profile were generated with the same parameter of rms height and correlation length.

After this, the reference simulation method described in Section II was used to simulate the upstream and downstream signals. This includes the static reference condition (dimensions, wedge angle, and placement), FE simulation setup, and flow simulation. The internal pipe surfaces in the FE simulation setup need to be replaced with the rough surfaces as defined in Figs. 13 and 14. Then, signal processing was carried out to calculate the flow velocity and the percentage error (due to internal rough surface) of this flow velocity compared with the reference flow velocity for each realization of a rough surface.

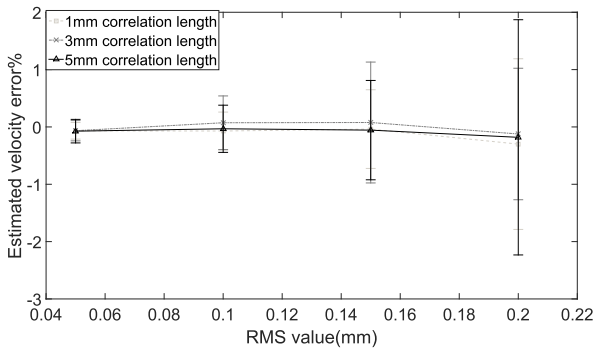


Fig. 15. Mean (marker) and standard deviation (error bar) of estimated velocity error as a function of surface roughness and rms values for different correlation lengths. For each point plotted, 10 realizations were used to estimate the mean and standard deviation that are shown in the graph.

This means for every rms and correlation length combination, 10 profiles and 10 systematic errors are generated. The reason for generating 10 different realizations is because depending on the actual pipe profile that ultrasound is transmitted through, the systematic errors will be different even if the profiles have the same rms value and correlation length. Therefore, one profile is not representative for this combination of parameters and several simulations need to be carried out to explore the range of systematic errors that can be expected.

The mean and standard deviation of 10 systematic errors generated from 10 realizations were then calculated for each rms and correlation length pair.

Fig. 15 shows the mean of the estimated flow velocity error as a function of correlation length and rms value. It can be seen that the mean of the errors is approximately 0 and the standard deviation is increasing as a function of rms. This means that although the mean error for roughness profiles with the same combination of parameters is 0, it is highly possible that for one particular pipe profile in the field, the systematic error generated will be nonzero. This proves that in this particular study, the mean error does not truly represent the influence of the roughness, but the standard deviation provides information on the average effect of roughness on the flow velocity measurement. This presentation is also consistent with that used by other authors to investigate the effect of scattering from rough surfaces [24].

The rms value of the internal pipe wall roughness clearly has a large impact on the uncertainties of clamp-on UFMs. Previous publications on the effect of roughness on ultrasonic measurements [25], [26] have described the main effects that are to be expected from the interaction of the ultrasonic beam with the rough surface. The relative size of the rms height compared with the wavelength of the ultrasonic wave is important. If the surface height varies by a considerable fraction of the ultrasonic wavelength, then the wave that enters the fluid from the surface of the steel can have spatially varying phase so that different components of the beam can constructively and destructively interfere with each other. This can change the amplitude and phase of the waves received and hence the apparent travel time. The correlation length controls the horizontal variation of the rough surface. If the correlation length is much smaller than the wavelength, then there can be many changes in the surface height over the size of the beam (assuming that the beam is a few wavelengths in size as is common for most transducers) and effects can average out. However, if the correlation length is of the order of the wavelength or longer, then there are only a few variations over the whole beam and the roughness will considerably distort the resulting signal. For a 1-MHz shear wave in steel, the wavelength is around 3 mm; therefore, the rms values and correlation length of the simulated surfaces are likely to introduce changes into the ultrasonic signals. It also happens to be that these surface roughness values are likely to be representative of the in-service pipes.

The standard deviation of the estimated flow velocity reaches approximately 2% for a moderately corroded pipe with rms 0.2 mm and correlation length 5 mm. This means that if clamp-on UFM on the pipe with these roughness parameters is used, the systematic errors that result purely from the roughness at the location of installation can be of the order of 2%. This is a large part of the uncertainties that are commonly attributed to clamp-on flowmeters by manufacturers (1%–5%).

## V. Discussion and Conclusion

The main objective of this paper is to determine the nonflow related effect of pipe wall roughness on uncertainties of clamp-on UFM. To achieve this, a reference simulation method based on reasonable assumptions was presented and experimentally verified. This method keeps the complexity of waves but simplifies the effect of flow. In this way, not only the computational burden is reduced but also the independent effect of pipe roughness on the uncertainties can be determined.

In this paper, only the internal pipe wall roughness was investigated as this parameter cannot be easily changed during the field measurement. The standard deviation of systematic errors caused by roughness (in this case, 2% for pipe with rms 0.2 mm and correlation length 5 mm) depends on the individual surface profile; however, the range of probable errors can clearly be identified by the results of this paper.

Experimental results for the uncertainty study of horizontal separation distance showed good agreement with the simulations. Therefore, it is believed that the additional complexity of the 3-D results will not affect the conceptual conclusion; however, it might affect the magnitude of the error that is to be expected.

Since manufacturers quote installation errors to be of the order of 1%–5%, these results show that surface roughness is an important parameter to consider in clamp-on UFM installation.

## Acknowledgment

The authors would like to thank ASEA Brown Boveri for providing useful background knowledge with respect to industrial flowmeters.

## References

[1] R. C. Baker, *Flow Measurement Handbook: Industrial Designs, Operating Principles, Performance, and Applications*. Cambridge, U.K.: Cambridge Univ. Press, 2000.

[2] L. C. Lynnworth and Y. Liu, "Ultrasonic flowmeters: Half-century progress report, 1955–2005," *Ultrasonics*, vol. 44, pp. e1371–e1378, Dec. 2006.
[3] O. Millán-Blasco, J. Salazar, J. A. Chávez, A. Turó-Peroy, and M. J. García-Hernández, "Zero-flow offset variation in ultrasonic clamp-on flowmeters due to inhomogeneity and nonlinearity of pipe materials," *IEEE Trans. Instrum. Meas.*, vol. 66, no. 11, pp. 2845–2851, Nov. 2017.
[4] V. D. Mahadeva, C. R. Baker, and J. Woodhouse, "Further studies of the accuracy of clamp-on transit-time ultrasonic flowmeters for liquids," *IEEE Trans. Instrum. Meas.*, vol. 58, no. 5, pp. 1602–1609, May 2009.
[5] J. Han, H. Liu, Y. Zhou, R. Zhang, and C. Li, "Studies on the transducers of clamp-on transit-time ultrasonic flow meter," in *Proc. 4th IEEE Int. Conf. Inf. Sci. Technol. (ICIST)*, Apr. 2014, pp. 180–183.
[6] M. L. Sanderson and H. Yeung, "Guidelines for the use of ultrasonic non-invasive metering techniques," *Flow Meas. Instrum.*, vol. 13, no. 4, pp. 125–142, 2002.
[7] M. Mori, K. Tezuka, and Y. Takeda, "Effects of inner surface roughness and asymmetric pipe flow on accuracy of profile factor for ultrasonic flow meter," in *Proc. 14th Int. Conf. Nucl. Eng.*, 2006, pp. 761–767.
[8] A. Calogirou, J. Boekhoven, and R. A. W. M. Henkes, "Effect of wall roughness changes on ultrasonic gas flowmeters," *Flow Meas. Instrum.*, vol. 12, no. 3, pp. 219–229, 2001.
[9] J. M. Szebeszczyk, "Application of clamp-on ultrasonic flowmeter for industrial flow measurements," *Flow Meas. Instrum.*, vol. 5, no. 2, pp. 127–131, 1994.
[10] M. Čermáková, J. Kriš, O. Čermák, and J. Bozikova, "Uncertainty in the measurements of clampon ultrasonic flowmeters," *Slovak J. Civil Eng.*, vol. 1, pp. 1–6, Apr. 2004.
[11] J. A. Ogilvy, *Theory of Wave Scattering From Random Rough Surfaces*. Bristol, U.K.: Institute of Physics Publishing Ltd., 1991.
[12] P. B. Nagy and L. Adler, "Surface roughness induced attenuation of reflected and transmitted ultrasonic waves," *J. Acoust. Soc. Amer.*, vol. 82, no. 1, p. 193, 1987.
[13] *American Society of Mechanical Engineers, Stainless Steel Pipe*, ASTM, Philadelphia, PA, USA, 2004.
[14] B. Iooss, C. Lhuillier, and H. Jeanneau, "Numerical simulation of transit-time ultrasonic flowmeters: Uncertainties due to flow profile and fluid turbulence," *Ultrasonics*, vol. 40, no. 9, pp. 1009–1015, 2002.
[15] *Abaqus Documentation 6.14*, Dassault Systémes Simulia Corp., Providence, RI, USA, 2014.
[16] M. B. Drozdz, "Efficient finite element modelling of ultrasound waves in elastic media," Ph.D. dissertation, Imperial College Sci. Technol. Med., London, U.K., 2008.
[17] J. Reyes, "Simulation and experimental validation of a transit time in an ultrasonic gas flow meter using air," in *Proc. IEEE ANDESCON*, Sep. 2010, pp. 1–6.
[18] P.-C. Eccardt, H. Landes, and R. Lerch, "Finite element simulation of acoustic wave propagation within flowing media," in *Proc. IEEE Ultrason. Symp.*, Nov. 1996, pp. 991–994.
[19] A. Luca, K. Fodil, and A. Zerarka, "Full-wave numerical simulation of ultrasonic transit-time gas flowmeters," in *Proc. IEEE Int. Ultrason. Symp. (IUS)*, Sep. 2016, pp. 1–4.
[20] M. Parrilla, J. J. Anaya, and C. Fritsch, "Digital signal processing techniques for high accuracy ultrasonic range measurements," *IEEE Trans. Instrum. Meas.*, vol. 40, no. 4, pp. 759–763, Aug. 1991.
[21] L. Svilainis and V. Dumbrava, "Analysis of the interpolation techniques for time-of-flight estimation," *Ultragarsas, Ultrasound*, vol. 63, no. 4, pp. 25–29, 2008.
[22] *Geometrical Product Specifications (GPS)—Surface Texture: Profile Method—Terms, Definitions and Surface Texture Parameters*, Standard EN ISO 4287:1998, Apr. 1997.
[23] *Process Design*, NORSOK Standard P-100, Norwegian Petroleum Industry, 2006, pp. 9–22.
[24] F. Cegla and A. Jarvis, "Modeling the effect of roughness on ultrasonic scattering in 2D and 3D," in *Proc. AIP Conf.*, vol. 1581. Feb. 2014, p. 595. [Online]. Available: https://aip.scitation.org/doi/pdf/10.1063/1.4864874
[25] D. Benstock, F. Cegla, and M. Stone, "The influence of surface roughness on ultrasonic thickness measurements," *J. Acoust. Soc. Amer.*, vol. 136, no. 6, pp. 3028–3039, 2014.
[26] A. Gajdacsi and F. Cegla, "The effect of corrosion induced surface morphology changes on ultrasonically monitored corrosion rates," *Smart Mater. Struct.*, vol. 25, no. 11, p. 115010, 2016.

**Xiaotang Gu** received the M.Eng. degree in mechanical engineering from Imperial College London, London, U.K., where he is currently pursuing the Ph.D. degree with the Dynamics and Non-Destructive Evaluation Group, Mechanical Engineering Department.

**Frederic Cegla** was born in Freiburg im Breisgau, Germany. He received the M.Eng. and Ph.D. degrees in mechanical engineering from Imperial College London, London, U.K, in 2002 and 2006, respectively.

He was a Founder of Permasense Ltd., Crawley, U.K., a spin out company and market leader in the field of wireless ultrasonic corrosion monitoring. He returned to Imperial College London after a short stay as a Post-Doctoral Research Fellow at the University of Queensland, Brisbane, QLD, Australia. He is currently a Senior Lecturer (Associate Professor) and an Engineering and Physical Sciences Research Council Research Fellow at the Non-Destructive Evaluation Group, Imperial College London. He has authored over 50 publications. He holds six patents. His current research interests include ultrasonic sensors, ultrasonic monitoring techniques, structural health monitoring, and ultrasonic manipulation of particles and bubbles.